Generation and Transmission of Optical Carrier Suppressed-Optical Differential (Quadrature) Phase-Shift Keying (OCS-OD(Q)PSK) Signals in Radio Over Fiber Systems

Qingjiang Chang, *Student Member, IEEE*, Yue Tian, *Student Member, IEEE, Student Member, OSA*, Junming Gao, Tong Ye, Qiang Li, *Student Member, IEEE*, and Yikai Su, *Senior Member, IEEE, Member, OSA*

***Abstract*—We propose and experimentally demonstrate generation of optical carrier suppressed-optical differential phase-shift keying (OCS-oDPSK) modulation format in radio-over-fiber (RoF) systems using one single-drive Mach–Zehnder modulator (MZM). This scheme realizes up-conversion of baseband data for downlink wireless service delivery, generation of remote local oscillator (LO) signal for down-conversion of uplink radio frequency (RF) signal, and remodulation of down-converted uplink data, thus lowering the cost of base stations (BSs) in full-duplex RoF systems. The proposed scheme is expected to be simple and compact due to the use of a single MZM. Furthermore, the OCS-oDPSK generation principle is extended to obtain an OCS-optical differential quadrature phase-shift keying (OCS-oDQPSK) signal by employing a dual-parallel MZM (DPMZM), which is useful to deliver multiple wireless services on the same RF carrier.**

***Index Terms*—Differential (quadrature) phase-shift keying D(Q)PSK), dual-parallel Mach–Zehnder modulator (DPMZM), optical carrier suppression (OCS), radio-over-fiber (RoF), single-drive Mach–Zehnder modulator (MZM).**

I. Introduction

THE convergence of wireless and optical fiber systems in an integrated platform has become a promising technique for providing broadband wireless access services with increased mobility and reduced cost [1]. In order to meet the requirement of high signal bandwidth and overcome the spectral congestion at the low frequency, future radio-over-fiber (RoF) systems would utilize millimeter-wave (MMW) frequency band for high-speed data delivery [2], [3]. However, the base station (BS) picocells have small coverage due to the high atmospheric attenuation in the MMW frequency band, which results in the need of many BSs to cover the operational area and thus greatly adds configuration cost of the overall system. Therefore, it is desirable to shift the system complexity and expensive devices to the central station (CS) to minimize the cost of BSs, which shows the advantages of concentrating the expensive equipments in the CS and sharing these equipments by all BSs. In this situation, the overall architecture design and the scheme for delivery of downlink and uplink services to realize full-duplex transmission play the key roles in the successful deployment in practical networks.

In RoF systems, for the downlink transmission, the generations of MMW for optical up-conversion of baseband data using external Mach–Zehnder modulator (MZM) or phase modulator in the CS have been demonstrated [4]–[16], where optical carrier suppression with optical amplitude shift keying (OCS-oASK) [7]–[14] or optical differential phase-shift keying (OCS-oDPSK) format [15], [16] is considered as a potential candidate technique due to the simplicity in system configuration and the good performance in long distance transmission. Moreover, the OCS technique can generate frequency-doubled MMW signal after beating in a photo-detector (PD), thus it has low bandwidth requirement for opto-electrical components.

On the other hand, realization of the uplink RoF transmission is more challenging. In some situations, a high-frequency radio frequency (RF) signal carrying data from the end users via an antenna has to be down-converted to baseband or intermediate frequency (IF) using a local oscillator (LO) signal, which is then modulated onto the optical carrier in the BS and sent back to the CS over the optical fiber. This requires a high-speed LO signal and a light source in the BS, thus resulting in difficulty in achieving the low-cost BSs. Many effective methods have been reported to provide solutions for the uplink transmission. Remote delivery of an unmodulated RF carrier from the CS was demonstrated to provide the LO signal for down-converting uplink signal [3], [17], [18]. In addition, other schemes were proposed to avoid the necessity for a light source in the BSs, such as reusing the optical carrier from the downlink [2], [3], [10]–[14], [19], employing a Fabry–Pérot laser diode with an optical bandpass filter at the CS [20], and remodulating the DPSK format [15], [16].

However, these previous schemes only realized either full duplex links without the generation of LO signal or unidirectional transmission with LO delivery, and the transmitter requires multiple discrete components. Simultaneous realization of bidirectional RoF links and remote LO delivery with cost-effective configuration has not been demonstrated.

Manuscript received January 30, 2008; revised May 27, 2008. Current version published October 10, 2008. This work was supported by the 863 High-Tech program (2006AA01Z255) and the Fok Ying Tung Fund (101067).

The authors are with the State Key Lab of Advanced Optical Communication Systems and Networks, Department of Electronic Engineering, Shanghai Jiao Tong University, Shanghai 200240, China (e-mail: yikaisu@sjtu.edu.cn).

Color versions of one or more of the figures in this paper are available online at http://ieeexplore.ieee.org.

Digital Object Identifier 10.1109/JLT.2008.927592

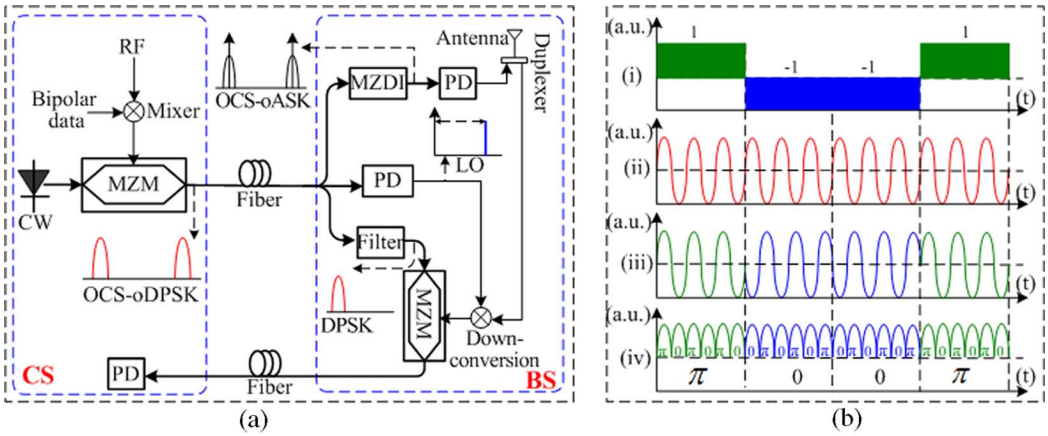

Fig. 1. (a) Schematic diagram for the generation and transmission of the OCS-oDPSK signal based on a MZM. (b) The operation principle for the generation of the OCS-oDPSK signal.

In this paper, we propose a simple yet effective OCS-oDPSK modulation scheme to simultaneously realize three key functions in RoF systems: 1) up-conversion of downlink baseband data to RF band; 2) generation of remote LO signal for down-converting uplink RF signal to baseband or IF; and 3) remodulation of uplink signal without the need of light source at the BSs. Moreover, in our scheme, the OCS-oDPSK is generated by using only one single-drive MZM (MZM), which exhibits the advantages of compact architecture, low cost, easy monitoring and control, and low insertion loss compared with previously proposed OCS-oDPSK transmitters [15], [16]. Based on the principle of OCS-oDPSK generation, an OCS-optical differential quadrature phase-shift keying (OCS-oDQPSK) signal is also obtained using a dual-parallel MZM (DPMZM) [21]. This format can deliver multiple RoF services [22], [23] on the same RF carrier and then improve the RF spectrum efficiency.

II. Operation Principle

The proposed configuration for OCS-oDPSK signal generation is shown in Fig. 1(a), where the CS consists of a MZM in push–pull operation and an electrical mixer. An alternating current (AC)-coupled bipolar baseband data (Fig. 1(b-i)) mixes with an RF signal [Fig. 1(b-ii)] to produce an electrical sub-carrier multiplexed (SCM) signal [Fig. 1(b-iii)], which can be expressed as

$$V_{\mathrm{SCM}}(t) = V_s \cdot \mathrm{data}(t) \cdot \sin(\omega_s t) \tag{1}$$

where data(t) [$= 1$ or -1] represents the AC-coupled random bit sequence, V_s is the amplitude of the mixed signal and ω_s is the angular frequencies of the RF signal. The MZM is driven by the mixed SCM signal plus the bias voltage, which can be described by

$$V(t) = \varepsilon V_\pi + \alpha V_\pi \cdot \mathrm{data}(t) \cdot \sin(\omega_s t) \tag{2}$$

where ε and α are the bias voltage of the modulator and the amplitude of the SCM signal normalized to the half-wave voltage V_π, respectively. The output field of the MZM can be given by

$$E_{\mathrm{out}}(t) = E_{\mathrm{in}}(t) \cdot \cos(\omega_c t) \cdot \cos\left\{\frac{\pi}{2}\left[\varepsilon + \alpha \cdot \mathrm{data}(t) \cdot \sin(\omega_s t)\right]\right\} \tag{3}$$

where ω_c and $E_{\mathrm{in}}(t)$ are the angular frequency and optical field amplitude of the input optical signal, respectively. When $\varepsilon = 1$, i.e., the MZM is biased at the transmission null, the even-order sidebands as well as the optical carrier can be suppressed, thus resulting in the generation of an OCS modulation format. An expansion of (3) with Bessel functions leads to an approximate expression for the output field as

$$E_{\mathrm{out}}(t) \approx AE_{\mathrm{in}}(t) \cdot \cos(\omega_c t) \cdot \sum_{n=1}^{\infty} J_{2n-1}\left(\frac{\pi}{2}\alpha \cdot \mathrm{data}(t)\right) \cdot \sin(\omega_s t) \tag{4}$$

where only the first-order sidebands are considered, the higher order sidebands are ignored due to the small optical powers. Equation (4) can be further described by

$$\begin{aligned} E_{\mathrm{out}}(t) &= AE_{\mathrm{in}}(t) \cdot \mathrm{sgn}\left(\mathrm{data}(t)\right) \cdot J_1\left(\frac{\pi}{2}\alpha \cdot |\mathrm{data}(t)|\right) \\ &\quad \cdot \sin(\omega_s t) \cdot \cos(\omega_c t) \\ &= AE_{\mathrm{in}}(t) \cdot \mathrm{sgn}\left(\mathrm{data}(t)\right) \cdot J_1\left(\frac{\pi}{2}\alpha\right) \\ &\quad \cdot \left[\cos(\omega_c - \omega_s)t - \cos(\omega_c + \omega_s)t\right]. \end{aligned} \tag{5}$$

Equation (5) shows that the envelope of the output signal is given by $AE_{\mathrm{in}}(t) \cdot J_1(\alpha) \cdot [\cos(\omega_c - \omega_s)t - \cos(\omega_c - \omega_s)t]$, which exhibits a periodic waveform in time domain [Fig. 1(b-iv)] and two tones in spectral domain. The phase of the optical output signal is determined by the sign of $\mathrm{sgn}(\mathrm{data}(t))$ and inverts instantaneously as the $\mathrm{data}(t)$ is changed. Between the bit "1" and the bit "-1", there is a phase jump at the transmission null. Consequently, the bit "1" corresponds to a carrier phase shift of π, while the bit "-1" leads to a carrier phase shift of 0, and both states have the same optical power, as shown in Fig. 1(b-iv). Therefore, the output signal is an OCS-oDPSK format.

The generated OCS-oDPSK is a two-tone signal, and each tone carries the same DPSK modulation data; thus, (5) can be further simplified to obtain the electrical field of the OCS-oDPSK

$$E_{\mathrm{out}}(t) = AE_{\mathrm{in}}(t) \cdot \{[\cos(\omega_c - \omega_s)t + \phi(t)] - [\cos(\omega_c + \omega_s)t + \phi(t)]\} \tag{6}$$

where $\phi(t)$ [$= 0$ or π] represents the instantaneous phase shifting of the DPSK data. Then the OCS-oDPSK is injected into a Mach–Zehnder delay interferometer (MZDI) to realize phase to intensity conversion. The MZDI has a relative time delay between its two arms equal to the bit period. Assuming that the coupling ratio of the two couplers in the MZDI is exactly 3 dB, the output electrical field from one output port of the MZDI can be expressed by

$$E_{\text{out\_MZDI}}(t) = \frac{1}{2}\left[E_{\text{out}}(t-T) + E_{\text{out}}(t)\right]. \tag{7}$$

Therefore, the two DPSK tones of the OCS-oDPSK are independently demodulated by the MZDI to generate two ASK signals, i.e., an OCS-oASK format is obtained and then an up-converted signal is produced after PD detection. One key aspect is that the central frequency of the MZDI must be matched to the wavelength of the OCS-oDPSK signal, and any frequency offset will cause a power penalty in the receiver sensitivity due to the phase mismatching at the output of the MZDI. In addition, the bit delay mismatch of the MZDI results in a penalty due to inter-symbol interference. Moreover, the low extinction ratio of the MZDI induces power difference between the two arms of the MZDI, which also causes amplitude fluctuations of the generated OCS-oASK signal. Since the DPSK signal is a phase-modulated format, one sideband of the OCS-oDPSK can be utilized as an optical carrier for remodulation of the down-converted uplink signal, which avoids the need of a light source for upstream signal modulation and thus eliminates complicated wavelength management in the BSs. On the other hand, if the OCS-oDPSK signal is directly detected by a PD, the two tones carried the same DPSK signals beat each other, one can obtain a clock signal that has twice the frequency of the RF signal, which can be used as the LO signal for the down-conversion of uplink RF signal. The obtained clock signal can be expressed as

$$V_{\text{out}}(t) = A^2 \left|E_{\text{in}}(t)\right|^2 \cdot \cos(2\omega_s t). \tag{8}$$

Using this simple and compact scheme, we realize the three key functions in RoF systems including the up-conversion of the downlink baseband data, the generation of remote LO signal, and the re-modulation of upstream data, by using a single MZM. Therefore, the system cost and complication could be potentially reduced.

We further extend the OCS-oDPSK generation principle to obtain an OCS-oDQPSK signal using a single DPMZM. The DPMZM [21] consists of a pair of x-cut LiNbO3 MZMs (MZMA, MZMB) embedded in the two arms of a main MZM structure. The two sub-MZMs have the same architecture and performance, and the main MZM combines the outputs of the two sub-MZMs. The schematic diagram of the OCS-oDQPSK signal generation is shown in Fig. 2, where the two sub-modulators are biased at the transmission null and driven by individual SCM modulating signals, respectively, to generate two independent OCS-oDPSK signals. Similarly, the SCM signal is produced by mixing a bipolar data with an RF signal. By adjusting the bias of the main modulator to ensure an optical $\pi/2$ phase difference between the outputs of the two submodulators, an OCS-oDQPSK signal is obtained, which

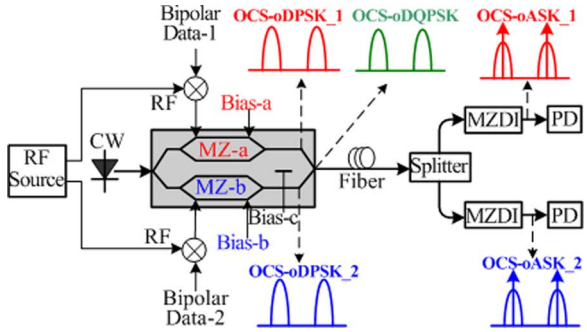

Fig. 2. Schematic diagram for the generation of the OCS-oDQPSK signal based on a single DPMZM.

is useful in providing multiple wireless access services on a common RF carrier in RoF systems. The two wireless signals carried at the common frequency band would interfere with each other in the same wireless link, resulting in worse performance of the received signals. However, this limitation can be resolved by using two antennas with orthogonal polarizations [24]. Furthermore, some optimization techniques of antenna polarization have been reported to minimize the interference through transmission [25]. Since the DPMZM is a commercial off-the-shelf device fabricated on a single chip, this scheme enables a cost-effective configuration for the generation of OCS-oDQPSK in RoF systems.

III. Experimental Results

We first perform an experiment to verify the feasibility of the proposed OCS-oDPSK scheme, as shown in Fig. 3. At the CS, a 10-GHz MZM is used to modulate a continuous wave (CW) light from a tunable laser at 1549.86 nm. The electrical SCM signal is obtained by mixing an AC-coupled 1.25-Gbps pseudorandom bit sequence (PRBS) baseband data of $2^{31} - 1$ with a 10-GHz RF signal, the waveform and the eye diagram are shown in Fig. 3(i) and (ii), respectively. In the experiment, a pulse pattern generator (PPG) (ANRITSU pulse pattern generator-MP1763c) is used to generate the 1.25-Gb/s data and provide the trigger signal for the oscilloscope. The 10-GHz clock is derived from an RF synthesizer (Agilent E8257D). To keep the synchronization between the PPG and the RF synthesizer, the PPG is set to take a 10-MHz reference from the output of the synthesizer. Then the electrical SCM signal is amplified to drive the MZM, which is biased at the transmission null to obtain an OCS-oDPSK signal with a 20-GHz repetition rate, the optical eye diagram and the optical spectrum are provided in Fig. 3(iii) and (iv), respectively. We use a fiber Bragg grating (FBG) to filter one sideband of the OCS-oDPSK signal for detection, the eye diagrams of the filtered tone before [Fig. 3(v)] and after [Fig. 3(vi)] demodulation by a 1-bit MZDI further verify that the generated signal is the OCS-oDPSK modulation format. The OCS-oDPSK signal is amplified by an erbium-doped fiber amplifier (EDFA) to a power level of ~8 dBm before transmission. Considering the fiber length and the power of the OCS-oDPSK signal, the nonlinear effects are not significant in this transmission system. A tunable optical filter (TOF) is employed to suppress the amplified spontaneous emission (ASE) noise. After transmission over 25-km standard single-

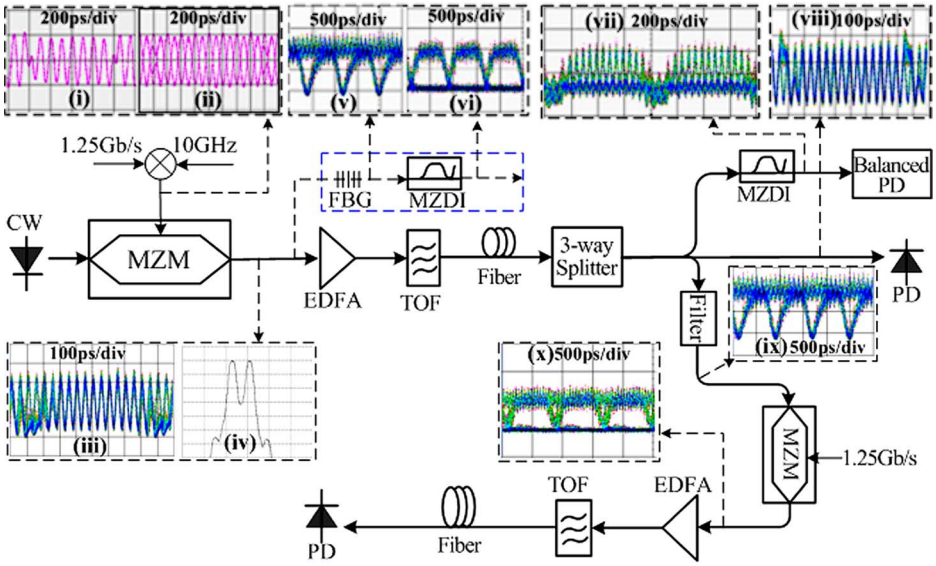

Fig. 3. Experimental setup for the generation and transmission of the OCS-oDPSK signal based on a MZM. Spectrum resolution: 0.07 nm; start wavelength: 1548.86 nm; stop wavelength: 1550.86 nm; X-axis scale: 0.2 nm/div, Y-axis scale: 5 dB/div. (i) The waveform of the mixed SCM signal. (ii) The electrical eye diagram of the mixed SCM signal. (iii) The optical eye diagram of the OCS-oDPSK signal. (iv) The optical spectrum of the OCS-oDPSK signal. (v) The optical eye diagram of one sideband of the OCS-oDPSK before demodulation. (vi) The optical eye diagram of one sideband of the OCS-oDPSK after demodulation. (vii) The optical eye diagram of the OCS-oDPSK after demodulation. (viii) The optical eye diagram before the PD. (ix) The optical eye diagram after the optical filter. (x)The optical eye diagram of the remodulated uplink signal.

mode fiber (SMF), at the BS, the OCS-oDPSK signal is divided into three parts by a three-way optical splitter, which consists of two 50:50 couplers and has a 1:1:2 splitting ratio for the downlink signal to be converted, the LO signal, and the uplink signal for remodulation, respectively. One part is demodulated by a 1-bit MZDI to convert the OCS-oDPSK signal into an OCS-oASK intensity signal, with the optical eye diagram after MZDI demodulation provided in Fig. 3(vii). The MZDI is made of two couplers, where the length difference between the two arms to realize 1-bit delay is ~15.96 cm for the 1.25-Gb/s DPSK data. Since the MZDI used in the experiment shows slight mismatched bit-delay between the two arms, there are some imperfections in the eye diagram. A balanced PD is required to convert the demodulated OCS-oDPSK signal to a 20-GHz electrical wireless signal for broadcasting through an antenna. In this particular demonstration, a 40-GHz high-speed PD is employed to realize single-end detection, thus generating a 20-GHz RF signal carrying the 1.25-Gb/s baseband data. The generated signal is input to an electrical spectrum analyzer (ESA) (ANRITSU MS2667C) for the measurement of the electrical spectrum, as shown in Fig. 4, where the spectrum range is from 18 to 22 GHz. Due to the lack of a fast-speed electrical mixer to down-convert the received 20-GHz RF signal to baseband, the signal is detected using a method similar to that in [15], where the bit-error-ratio (BER) measurements are performed by detecting the upper-sideband component employing a 2.5-GHz low-speed PD. Fig. 5 shows the measured BER performances and the electrical eye diagram after transmission of 25-km SMF, where the power penalty of the downlink OCS-oDPSK signal is less than 0.5 dB. In practice, however, at the receiver, the 20-GHz wireless signal should be down-converted to baseband by mixing with a 20-GHz LO signal [2] for BER detection. We compare the difference of the BER performances in the receivers between filtering one side-band and using a mixer for the down-conversion [2] by VPI simulation software. Simulation results show that the recovered signals based on the two detection methods have similar quality, and the difference of the penalties for the signal through 25-km transmission with the two detection schemes are negligible.

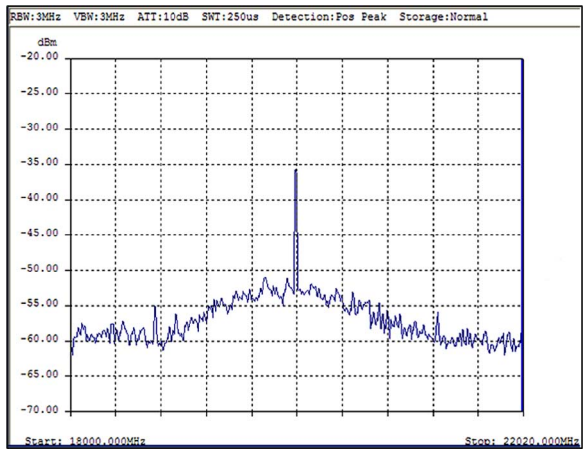

Fig. 4. Electrical spectrum of the 20-GHz RF signal carrying the 1.25-Gb/s baseband data.

The second part is directly detected by the 40-GHz PD to generate a LO signal, the eye diagram before the PD is indicated in Fig. 3(viii). Since the generated OCS-oDPSK has residual amplitude modulations, the intensity dips of the DPSK format would be translated to the electrical domain, which result in harmonic components and affect the spectrum purity of the obtained LO signal. Fig. 6 shows the electrical spectrum from 0 GHz to 25 GHz, where the amplitude of the harmonics

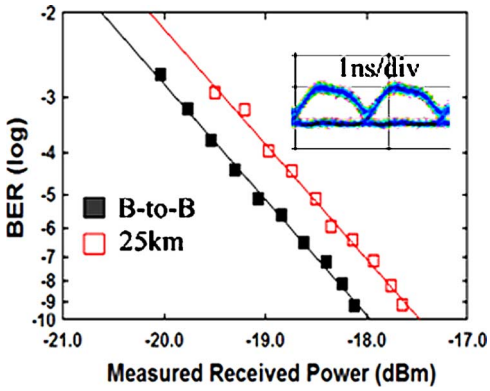

Fig. 5. BER curves and the electrical eye diagram of the downlink RoF signal.

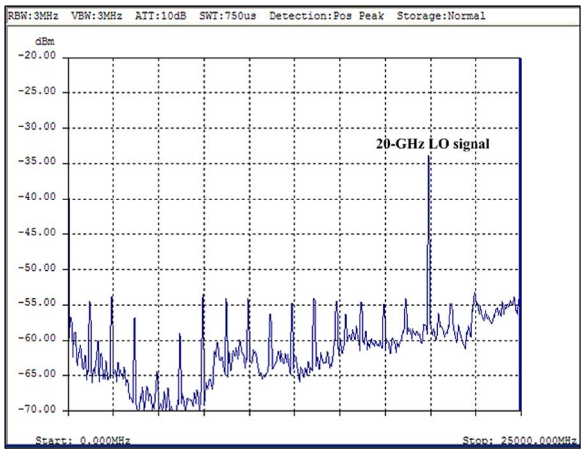

Fig. 6. Electrical spectrum of the generated 20-GHz LO signal.

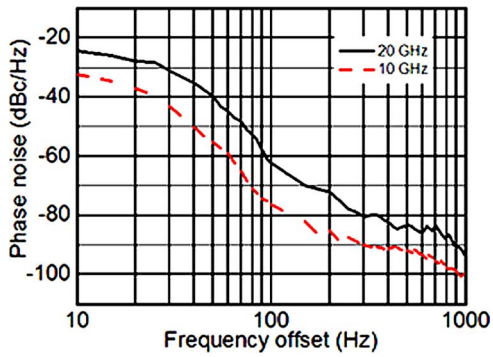

Fig. 7. Phase noise of the received 20-GHz clock signal.

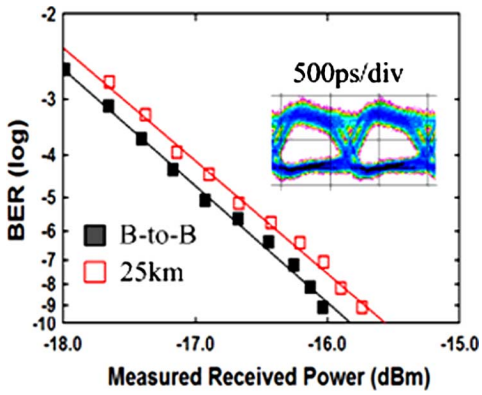

Fig. 8. BER curves and the electrical eye diagram of the uplink remodulated ASK signal.

are 20-dB lower than the generated LO signal. Moreover, a narrow-band filter should be used to further improve the spectrum purity of the LO signal. Fig. 7 indicates the phase noise performance of the received 20-GHz signal, relative to the 10-GHz clock from the low-noise RF synthesizer (Agilent E8257D). The phase noise is obtained by the ESA with a resolution of 30 Hz. The results show that the received 20-GHz clock signal has a phase noise ~ -93 dBc/Hz at 1-kHz offset. Compared to the 10-GHz signal with low phase noise of ~ -100 dBc/Hz at 1-kHz offset, $\sim$7-dB phase noise degradation is observed. Theoretically, a frequency-doubled signal has a phase noise degradation of about $10\text{Log}_{10}(2^2) = 6$ dB [26]. Therefore, the measurements show good phase-noise performance of the received 20-GHz clock signal, which is close to the level of the RF synthesizer if the frequency doubling process is taken into account.

The third part is injected into an optical filter (3-dB bandwidth of $\sim$0.114 nm) to filter one sideband, which is remodulated by a 1.25-Gb/s PRBS baseband data with a word length of $2^{31}-1$ to produce an ASK format, the optical eye diagram before and after the uplink MZM are provided in Fig. 3(ix) and Fig. 3(x), respectively. In real network implementations, a diplexer connected with the antenna is needed to broadcast up-converted downstream wireless signals and receive upstream RF signals at the BS. The baseband upstream data is obtained by down-converting the RF signals from the diplexer. For the remodulated uplink ASK signal, the power penalty is $\sim$0.3 dB, and the electrical eye diagram is shown in inset of Fig. 8. Compared with the downlink BER performances, the uplink signal experiences $\sim$2-dB penalty, which could be attributed to the additional ASE noise from another EDFA. Moreover, the downlink signal is demodulated by a 1.25-Gb/s narrow-band MZDI filter, while the uplink signal passes through an optical filter with a 3-dB bandwidth of $\sim$0.114 nm, thus resulting in more noise power at the uplink receiver and degrading the receiver sensitivity of the uplink signal.

Therefore, a full-duplex RoF system with remote LO generation is realized, where the downlink signal transmission, the LO signal generation, and the uplink remodulation are simultaneously demonstrated.

We also demonstrate the generation of the OCS-oDQPSK signal using one 10-GHz DPMZM (COVEGA Mach-10060, 5.8-dB insertion loss), as shown in Fig. 9. The two submodulators are biased at the transmission null and driven by two independent SCM signals to generate the OCS-oDPSK format, respectively. The SCM is obtained by mixing the AC-coupled 1.25-Gb/s data with a 10-GHz RF signal. The bias of the main MZM is adjusted to obtain $\pi/2$ phase difference between the two OCS-oDPSK tributaries, the optical eye diagrams, and the spectra are shown in insets of Fig. 9, respectively. Then the two OCS-oDPSK tributaries are combined to achieve an OCS-oDQPSK signal at the output port of the main modulator. The optical eye diagram of the generated OCS-oDQPSK with

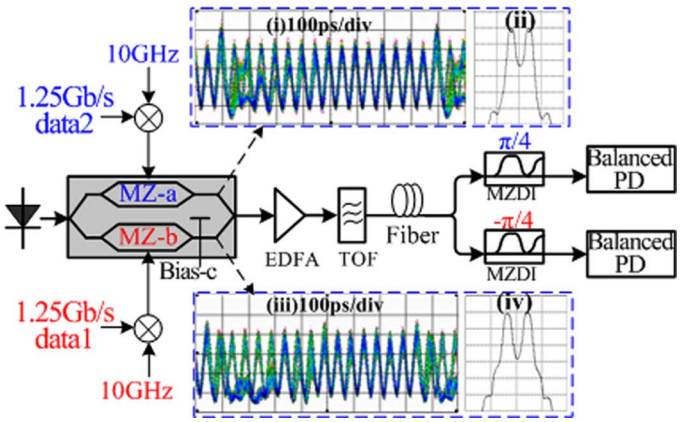

Fig. 9. Experimental setup for the generation of OCS-oDQPSK based on one DPMZM. Spectrum resolution: 0.07 nm; start wavelength: 1548.86 nm; stop wavelength: 1550.86 nm; X-axis scale: 0.2 nm/div, Y-axis scale: 5 dB/div. (i) The optical eye diagram of the in-phase OCS-oDPSK tributary. (ii) The optical spectrum of the in-phase OCS-oDPSK tributary. (iii) The optical eye diagram of the quadrature-phase OCS-oDPSK tributary. (iv) The optical spectrum of the quadrature-phase OCS-oDPSK tributary.

20-GHz repetition rate is indicated in Fig. 10(i). After amplified by an EDFA and 25-km SMF transmission, the signal is received by an OCS-oDQPSK receiver. For OCS-oDQPSK receivers, two 1-bit delay MZDIs with two separate balanced PDs are generally required to simultaneously demodulate the two tributaries. Here, we utilize a single MZDI to demodulate each tributary by adjusting the differential optical phase between the two MZDI arms to be $\pi/4$ or $-\pi/4$ [27]. Since the eye diagrams after MZDI demodulation between the two tributaries are basically identical, we only show the eye diagram of one tributary, as provided in Fig. 10(ii). There are some ripples in the eye diagram due to the imperfect MZDI. Using a detection method similar to that for the OCS-oDPSK signal, one sideband of the demodulated OCS-oDQPSK is filtered by an optical filter from one output port of the de-modulator, which is connected to a single 2.5-GHz low-speed PD without the use of a balance receiver, the optical and electrical eye diagrams are shown in Fig. 10(iii) and (iv), respectively. Fig. 11 gives the BER results of the in-phase and quadrature tributaries, respectively. For the two data channels, less than 0.3-dB power penalties after 25-km transmission are obtained.

IV. Conclusion

We have proposed a simple and effective scheme to obtain the OCS-oDPSK signal using only a MZM driven by a SCM signal. We experimentally demonstrated that the OCS-oDPSK can be used to simultaneously realize the up-conversion of baseband data for downlink wireless service delivery, the generation of remote LO signal, and the remodulation of the uplink data. Based on the OCS-oDPSK generation principle, an OCS-oDQPSK signal is also obtained using a DPMZM for simultaneously delivering multiple RoF services at the common RF carrier. The results show that our scheme provides a candidate technique to enable a compact and cost-effective configuration for future RoF applications.

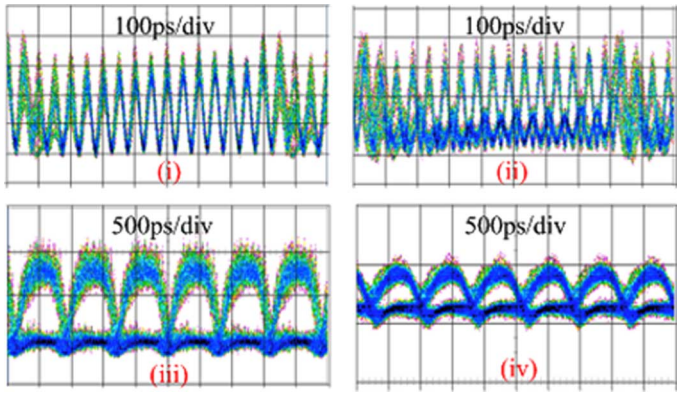

Fig. 10. (i) Optical eye diagram of the OCS-oDQPSK. (ii) The optical eye diagram of OCS-oDQPSK after MZDI de-modulation. (iii) The optical eye diagram of filtered one sideband after MZDI demodulation. (iv) The electrical eye diagram of filtered one sideband after PD detection.

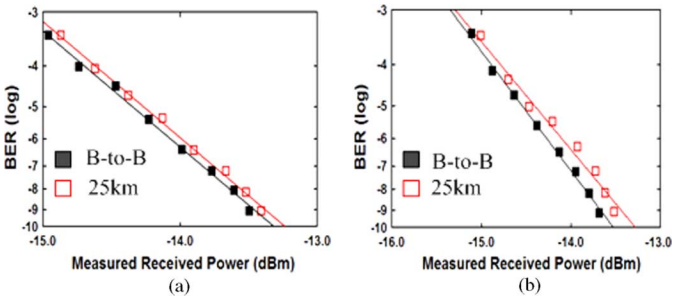

Fig. 11. BER curves of the OCS-oDQPSK. (a) In-phase data channel. (b) Quadrature data channel.

Acknowledgment

The authors would like to thank Dr. X. Wang of the Institute of Wireless Communication Technology and Ph.D. student B. Liu of the Center for Microwave and RF Technologies for their useful discussions.

References

[1] D. Wake, M. Webster, G. Wimpenny, K. Beacham, and L. Crawford, "Radio over fiber for mobile communications," in *Proc. IEEE Int. Topical Meeting Microw. Photon. (MWP 2004)*, Oct. 2004, pp. 157–160.

[2] Z. Jia, J. Yu, and G. K. Chang, "A full-duplex radio-over-fiber system based on optical carrier suppression and reuse," *IEEE Photon. Technol. Lett.*, vol. 18, no. 16, pp. 1726–1728, Aug. 2006.

[3] A. Kaszubowska, L. Hu, and L. P. Barry, "Remote down conversion with wavelength reuse for the radio/fiber uplink connection," *IEEE Photon. Technol. Lett.*, vol. 18, no. 4, pp. 562–564, Feb. 2006.

[4] G. H. Smith, D. Novak, and Z. Ahmed, "Overcome chromatic-dispersion effects in fiber-wireless systems incorporating external modulators," *IEEE Trans. Microw. Theory Tech.*, vol. 45, no. 8, pt. 2, pp. 1410–1415, Aug. 1997.

[5] U. Glies, S. Norskov, and T. N. Nielsen, "Chromatic dispersion in fiber-optic microwave and millimeter-wave links," *IEEE Trans. Microw. Theory Tech.*, vol. 44, no. 10, pt. 1, pp. 1716–1724, Oct. 1996.

[6] M. Attygalle, C. Lim, G. J. Pendock, A. Nirmalathas, and G. Edvell, "Transmission improvement in fiber wireless links using fiber bragg gratings," *IEEE Photon. Technol. Lett.*, vol. 17, no. 1, pp. 190–192, Jan. 2005.

[7] J. Yu, Z. Jia, L. Yi, Y. Su, G.-K. Chang, and T. Wang, "Optical millimeter-wave generation or up-conversion using external modulators," *IEEE Photon. Technol. Lett.*, vol. 18, no. 1, pp. 265–267, Jan. 2006.

[8] C. Lin, W. Peng, and P. Peng, "Simultaneous generation of baseband and radio signals using only one single-electrode Mach-Zehnder modulator with enhanced linearity," *IEEE Photon. Technol. Lett.*, vol. 18, no. 23, pp. 2481–2483, Dec. 2006.
[9] G.-K. Chang, J. Yu, Z. Jia, and J. Yu, "Novel optical-wireless access network architecture for simultaneously providing broadband wireless and wired services," presented at the OFC, Los Angeles, CA, 2006, paper OFM1, unpublished.
[10] L. Chen, H. Wen, and S. Wen, "A radio-over-fiber system with a novel scheme for millimeter-wave generation and wavelength reuse for up-link connection," *IEEE Photon. Technol. Lett.*, vol. 18, no. 19, pp. 2056–2058, Oct. 2006.
[11] L. Chen, Y. Shao, X. Lei, H. Wen, and S. Wen, "A novel radio-over fiber system with wavelength reuse for upstream data connection," *IEEE Photon. Technol. Lett.*, vol. 19, no. 6, pp. 387–389, Mar. 2007.
[12] J. Yu, Z. Jia, T. Wang, and G.-K. Chang, "A novel radio-over-fiber configuration using optical phase modulator to generate an optical mm-wave and centralized lightwave for uplink connection," *IEEE Photon. Technol. Lett.*, vol. 19, no. 3, pp. 140–142, Feb. 2007.
[13] A. Wiberg, P. P. Millán, M. V. Andrés, P. A. Andrekson, and P. O. Hedekvist, "Fiber-optic 40 GHz mm-wave link with 2.5 Gb/s data transmission," *IEEE Photon. Technol. Lett.*, vol. 17, no. 9, pp. 1938–1940, Sep. 2005.
[14] L. Chen, S. Wen, Y. Li, J. He, H. Wen, Y. Shao, Z. Dong, and Y. Pi, "Optical front-ends to generate optical millimeter-wave signal in radio-over-fiber systems with different architectures," *J. Lightw. Technol.*, vol. 25, no. 11, pp. 3381–3397, Nov. 2005.
[15] Q. Chang, H. Fu, and Y. Su, "Simultaneous generation and transmission multi-band signals and upstream data in a bidirectional radio over fiber system," *IEEE Photon. Technol. Lett.*, vol. 20, no. 3, pp. 181–183, Feb. 2008.
[16] Z. Jia, J. Yu, D. Boivin, M. Haris, and G.-K. Chang, "Bidirectional RoF links using optically up-converted DPSK for downstream and remodulated OOK for upstream," *IEEE Photon. Technol. Lett.*, vol. 19, no. 9, pp. 653–655, May 2007.
[17] C. Lim, A. Nimarthalas, D. Novak, R. Waterhouse, and G. Yoffe, "Millimeter-wave broad-band fiber-wireless system incorporating baseband data transmission over fiber and remote LO delivery," *J. Lightw. Technol.*, vol. 18, pp. 1355–1363, Oct. 2000.
[18] G. H. Smith and D. Novak, "Broadband millimeter-wave fiber-radio network incorporating remote up/downconversion," in *Proc. IEEE MTT-S Int. Microw. Symp. Dig.*, Baltimore, MD, 1998, pp. 1509–1512.
[19] A. Nirmalathas, D. Novak, C. Lim, and R. B. Waterhouse, "Wavelength reuse in the WDM optical interface of a millimeter-wave fiber-wireless antenna base station," *IEEE Trans. Microw. Theory Tech.*, vol. 49, no. 10, pp. 2006–2009, Oct. 2001.
[20] H.-H. Lu, A. S. Patra, W.-J. Ho, P.-C. Lai, and M.-H. Shiu, "A full-duplex radio-over-fiber transport system based on FP laser diode with OBPF and optical circulator with fiber Bragg grating," *IEEE Photon. Technol. Lett.*, vol. 19, no. 20, pp. 1652–1654, Oct. 2007.
[21] K. Higuma, S. Oikawa, Y. Hashimoto, H. Nagata, and M. Izutsu, "X-cut lithium niobate optical single-sideband modulator," *Electron. Lett.*, vol. 37, no. 8, pp. 515–516, Apr. 2001.
[22] X. Qian, T. Lin, R. V. Penty, and I. H. White, "Novel SOA-based switch for multiple radio-over-fiber service applications," presented at the OFC, Los Angeles, CA, 2006, paper JTHB 24, unpublished.
[23] M. Fujise and H. Harada, "An experimental study on multi-service radio on fiber transmission system for ITS road-vehicle communications," in *Proc. MWP '99 Melbourne*, Australia, vol. 1, pp. 261–264.
[24] L. Matabishi, "Theoretical implementation of antenna polarization to improve the reduction of co-channel interference in mobile cellular systems," in *Proc. IEEE Int. Microw., Antenna, Propag. EMC Technologies for Wireless Commun. (MAPE'05)*, Aug. 2005, vol. 1, pp. 431–433.
[25] D. P. Stapor, "Optimal receive antenna polarization in the presence of interference and noise," *IEEE Trans. Antennas Propag.*, vol. 43, no. 5, pp. 473–477, May 1995.
[26] Q. Wang, H. Rideout, F. Zeng, and J. Yao, "Millimeter-wave frequency tripling based on four-wave mixing in a semiconductor optical amplifier," *IEEE Photon. Technol. Lett.*, vol. 18, no. 23, pp. 2460–2462, Dec. 2006.
[27] H. Kim and P. J. Winzer, "Robustness to laser frequency offset in direct-detection DPSK and DQPSK systems," *J. Lightw. Technol.*, vol. 21, no. 9, pp. 1887–1891, Sep. 2003.

Qingjiang Chang (S'07) received the B.S. degree from Shandong University of Science and Technology, Qingdao, China, in 2001 and the M.S. degree from the Jiangnan University, Wuxi, China, in 2006. He is currently pursuing the Ph.D. degree at Shanghai Jiao Tong University, Shanghai, China.

His research interests include microwave photonics and passive optical networks.

Yue Tian (S'07) received the B.S. degree in communication engineering from Shanghai Jiao Tong University (SJTU), Shanghai, China, in 2006, where he is currently working toward the M.S. degree in communication and information system.

Since October 2005, he has been with the State Key Laboratory of Advanced Optical Communication Systems and Networks, SJTU. His research interests include the optical virtual private networks, optical access networks, and modulation formats.

Mr. Tian is a student member of IEEE and OSA. He serves as a Vice-President of Shanghai Jiao Tong University Student Chapter of OSA.

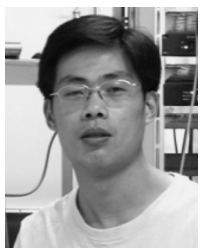

Junming Gao received the B.S. degree from Jilin University, Changchun, China, in 2006. He is currently pursuing the M.S. degree at Shanghai Jiao Tong University, Shanghai, China.

His research area includes 100-G ultra-high-speed transmission systems and time-domain wavelength interleaved network.

Tong Ye received the B.S. and M.S. degrees from the University of Electronic Science and Technology of China, Chengdu, in 1998 and 2001, respectively, and the Ph.D. degree in electronics engineering from Shanghai Jiao Tong University, Shanghai, China, in 2005.

He was with Chinese University of Hong Kong for one and half years before he joined the Shanghai Jiao Tong University as a Lecturer in 2006.

His research interests mainly include high-speed transmission, optical signal processing, and physical-layer optical networking.

Qiang Li (S'07) received the B.S. and the M.S. degrees from Harbin Institute of Technology, Harbin, China, in 2005 and 2007, respectively. He is currently pursuing the Ph.D. degree at Shanghai Jiao Tong University, Shanghai, China.

His research interests include slow light delay line and storage, and optical information processing in silicon waveguides.

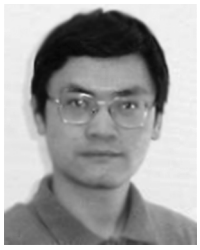

Yikai Su (M'01–SM'07) received the B.S. degree from the Hefei University of Technology, Hefei, China, in 1991, the M.S. degree from the Beijing University of Aeronautics and Astronautics, Beijing, China, in 1994, and the Ph.D. degree in electronics engineering from Northwestern University, Evanston, IL, in 2001.

He was with Crawford Hill Laboratory of Bell Laboratories for three years before he joined Shanghai Jiao Tong University, Shanghai, China, as a Full Professor in 2004. He became the associate Department Chair of Electronic Engineering in 2006. His research areas cover ultrahigh-speed transmission and modulation formats, optical signal processing, and enabling devices and modules. He has $\sim$150 publications in prestigious international journals and conferences, including $\sim$40 IEEE PHOTONICS TECHNOLOGY LETTERS papers, more than 20 invited conference presentations, and eight postdeadline papers. He holds three U.S. patents with over ten U.S. or Chinese patents pending.

Prof. Su serves as a Guest Editor of IEEE JSTQE, a Co-Chair of Workshop on Optical Transmission and Equalization (WOTE) 2005, ChinaCom2007 symposium, IEEE/OSA AOE 2007 slow light workshop, Asia Pacific Optical Communications (APOC) 2008 SC3, and a Technical Committee Member of Opto-Electronics and Communications Conference (OECC) 2008, the Conference on Laser and Electro-Optics (CLEO) Pacific Rim (PR) 2007, IEEE Lasers and Electro-Optics Society (LEOS) summer topical meeting 2007 on ultrahigh-speed transmission, IEEE Lasers and Electro-Optics Society (LEOS) 2005–2007, BroadNets2006, the Asia-Pacific Optical Communications (APOC) Conference 2005, and the International Conference on Optical Communications and Networks (ICOCN) 2004.